Applied Mathematics & Information Sciences
An International Journal

http://dx.doi.org/10.18576/amis/200319

Statistical Inference and Applications of the Inverse Power Half-Logistic Distribution in Reliability Analysis

Abdallah G. Bani-Saleh[1], *Dina A. Ramadan*[1,*], *B. S. El-Desouky*[1], *and Mahmoud M. El-Awady*[2]

[1]Department of Mathematics, Faculty of Science, Mansoura University, Mansoura, Egypt
[2]Misr Higher Institute for Commerce and Computers, Mansoura, Egypt

Received: 7 Feb. 2026, Revised: 21 Mar. 2026, Accepted: 23 Apr. 2026
Published online: 1 May 2026

Abstract: This paper proposes a new two-parameter lifetime model, referred to as the Inverse Power Half-Logistic ($IPHL$) distribution, which is constructed by applying an inverse power transformation to the power half-logistic distribution. The $IPHL$ model demonstrates high flexibility and is capable of modeling various hazard rate shapes, including increasing, decreasing, unimodal, and bathtub-shaped patterns, making it suitable for reliability and survival data analysis. Key statistical and reliability properties of the proposed distribution are derived, such as the density and distribution functions, survival and hazard functions, moments, quantile function, mean residual life, Rényi entropy, and stress–strength reliability measure. Parameter estimation is carried out using several methods, including maximum likelihood estimation (MLE), maximum product spacing (MPS), and least squares estimation (LSE). In addition, Bayesian estimation (BE) is performed using Markov Chain Monte Carlo ($MCMC$) techniques. Along with MPS and LSE methods. Interval estimation is addressed through asymptotic, bootstrap, and Bayesian credible intervals. A Monte Carlo simulation study is conducted to assess and compare the performance of the proposed estimators. Furthermore, the applicability of the $IPHL$ distribution is illustrated using two real lifetime datasets, where its performance is compared with several competing inverse models. The results indicate that the $IPHL$ distribution provides improved goodness-of-fit and greater modeling flexibility, confirming its effectiveness for practical reliability applications.

Keywords: Inverse Power Half-Logistic distribution; Lifetime modeling; Reliability analysis; Survival analysis; Parameter estimation; Bayesian inference; Markov Chain Monte Carlo; Monte Carlo simulation; Goodness-of-fit; Real data applications.

1 Introduction

Lifetime data analysis and reliability modeling play a fundamental role in applied statistics due to their wide-ranging applications in engineering, biomedical sciences, actuarial studies, pharmaceutical research, and industrial quality control. These fields are primarily concerned with modeling the time until the occurrence of a specific event, such as system failure, component breakdown, patient recovery, or mortality. Consequently, selecting an appropriate probabilistic model is essential for accurate statistical inference, reliable prediction, and effective decision-making.

Classical lifetime distributions, including the exponential, Weibull, Rayleigh, and logistic models, have been extensively used because of their mathematical simplicity and analytical tractability. However, empirical evidence has shown that these traditional models often lack sufficient flexibility to adequately describe real-world lifetime data, which frequently exhibit skewness, heavy tails, and non-monotonic hazard rate behaviors such as unimodal or bathtub-shaped failure rates. These limitations have motivated the development of more flexible distributional models capable of capturing complex data characteristics.

In this context, inverse distributions have received increasing attention in the literature on survival analysis and reliability theory. Inverse models have proven particularly effective for analyzing lifetime data associated with long survival times, early-life failures, or decreasing and non-standard hazard rate patterns. Notable examples include the inverse exponential distribution, the inverted gamma distribution Lin et al. [28], the generalized inverse Lindley distribution motivated by the work of Sharma et al. [37] and the inverse Gompertz distribution motivated by the work of Eliwa et al. [16].

* Corresponding author e-mail: dinaramadan21@mans.edu.eg

These models have demonstrated strong performance in various reliability and biomedical applications. Several related inverse lifetime models have also been discussed in recent studies [9,10,13,19].

Among modern approaches for constructing flexible inverse lifetime models, the inverse power transformation has emerged as a powerful and systematic technique. This method introduces an additional shape-controlling parameter through an inverse power transformation of the baseline random variable, significantly enhancing the flexibility of the resulting distribution. By adjusting this parameter, a wide range of density shapes and hazard rate behaviors can be obtained. The inverse power approach has been successfully employed in the development of several recent lifetime distributions, such as the inverse power Lomax distribution Al-Marzouki et al. [5], the inverse power Maxwell distribution Al-Kzzaz and Abd El-Monsef [4], and the inverse-power logistic-exponential distribution proposed by Al Sobhi [6] other related models that have shown superior fitting performance for insurance, medical, and reliability data, including heavy-tailed radiation and insurance datasets as discussed by Alghamdi et al. [3], see [7].

On the other hand, the half-logistic distribution and its extensions constitute an important class of lifetime models due to their desirable mathematical properties and ability to capture asymmetric lifetime behaviors. Several generalizations of the half-logistic family have been proposed in the literature, including the power half-logistic distribution by Krishnarani [26], inverse and generalized half-logistic-type models by Al-Marzouki et al. [5] and Kamnge and Chacko [22], as well as the exponentiated half-logistic Weibull distribution with reliability applications [45]. More recently, half-logistic-based models have been employed in broader reliability settings, including multicomponent stress–strength analysis under progressive first-failure censoring [43] and optimal life-testing design under adaptive progressive censoring [44]. Parallel developments in lifetime and reliability modeling have also emphasized flexible distribution construction and advanced inferential methodologies under complex censoring schemes, including generalized power lifetime models [40], inverse power lifetime distributions [41], multicomponent stress–strength reliability inference [47], competing-risk regression analysis [42], flexible deformation-based lifetime models [46], and dependent competing-risk modeling [48]. Despite these important developments, there remains a need for more flexible models that combine the strengths of inverse distributions with the adaptability offered by inverse power transformations. Additional half-logistic extensions were also investigated in the literature [11,31,32].

The motivation for this study stems from the growing need for flexible lifetime models capable of accurately describing complex real-world data encountered in reliability engineering and biomedical research. Many commonly used lifetime distributions fail to capture essential data features such as skewness, heavy tails, and non-monotonic hazard rate behaviors, which frequently arise in practice. Although inverse lifetime distributions and half-logistic-based models have been shown to improve modeling performance, existing models still exhibit limitations in flexibility and goodness-of-fit when applied to diverse datasets. Moreover, recent developments using inverse power transformations have demonstrated substantial potential for enhancing distributional adaptability, yet their application to half-logistic-based models remains limited. These considerations motivate the development of the $IPHL$ distribution, which aims to combine the advantages of inverse modeling and the inverse power transformation to provide a more versatile and robust tool for lifetime data analysis.

Accordingly, this study introduces the $IPHL$ distribution and investigates its statistical, reliability, and inferential properties. The main contributions of this work include deriving the probability density function (PDF), cumulative distribution function (CDF), quantile function, moments, reliability measures, order statistics, mean residual life function, Rényi entropy, and the stress-strength parameter. Several parameter estimation methods are also considered, including MLE, MPS, LSE, and BE. The finite-sample performance of these estimators is evaluated through simulation studies.

An important aspect of this study is the use of real-life datasets to demonstrate the practical relevance and applicability of the proposed $IPHL$ distribution. The analyzed datasets represent typical time-to-event data arising in biomedical and reliability contexts, including patient relief times and radiation-related exposure durations. Such data are characterized by positive support, skewness, and complex hazard rate behavior, which often pose challenges for classical lifetime models. By applying the $IPHL$ distribution to these datasets, the study highlights its ability to capture the underlying data structure more accurately than several well-established inverse lifetime models. The empirical results, supported by standard goodness-of-fit measures and graphical diagnostics, demonstrate the effectiveness and practical relevance of the proposed model for real-world lifetime data.

The remainder of this paper is organized as follows. Section 2 derives the PDF, CDF, and quantile function. Section 3 studies the statistical properties and reliability measures, including moments, survival function, hazard function, reversed hazard rate function, moment generating function (MGF), quantile and median, mode, order statistics, mean residual life function (MRL), Rényi entropy, and the stress-strength parameter. Section 4 develops parameter estimation methods, namely MLE, MPS, LSE, and BE under different loss functions, and constructs bootstrap confidence intervals. Section 5 reports the simulation results used to assess estimator performance. Section 6 presents applications to real-world lifetime data and compares the $IPHL$ model with benchmark distributions. Finally, Section 7 concludes the paper.

2 Inverse Power Half-Logistic Distribution

In this section, we introduce and develop a new probability distribution, referred to as the IPHL distribution. This model is constructed by applying an inverse power transformation to the baseline Power Half-Logistic distribution in order to enhance its flexibility for modeling lifetime and reliability data.

The PHL distribution is a well-established continuous probability distribution that emerges as a truncated and scaled form of the standard logistic distribution. It is defined on the positive real line and is frequently employed in the context of reliability analysis, lifetime data modeling, and the characterization of skewed and asymmetric phenomena. By restricting the support of the logistic distribution to the interval $(0,\infty)$, the PHL distribution retains analytical tractability while exhibiting a strictly increasing hazard rate function. This property makes it suitable for modeling failure-time processes in which the instantaneous failure rate escalates over time. Applications of the PHL distribution include the modeling of aging mechanical components, biological degradation processes, and other systems exhibiting time-accelerated failure behavior [26].

Definition 1. If T is a random variable distributed according to the PHL distribution characterized by a scale parameter α, then the CDF, denoted by $F_{\mathrm{PHL}}(t;\alpha)$, and the corresponding PDF, denoted by $f_{\mathrm{PHL}}(t;\alpha)$, are expressed as follows:

$$f_{\mathrm{PHL}}(t;\alpha)=\frac{2\alpha e^{-\alpha t}}{(1+e^{-\alpha t})^2},\qquad t,\alpha>0, \tag{1}$$

$$F_{\mathrm{PHL}}(t;\alpha)=\frac{1-e^{-\alpha t}}{1+e^{-\alpha t}},\qquad t,\alpha>0. \tag{2}$$

In this context, the parameter α serves as a scale parameter, influencing the distribution's dispersion or spread.

The suggested distribution's construction is based on using the inverse power transformation on the CDF and PDF of the PHL distribution. This transformation is defined as:

$$X=T^{-1/\beta},$$

where T represents the original variable and β serves as a shape-controlling parameter. Modifying β allows the transformation to substantially change the distributional shape, thereby enhancing the model's adaptability to various data structures.

In the following, we derive the CDF and PDF of the proposed IPHL distribution. The derivation is based on the inverse power transformation applied to the baseline PHL distribution, whose PDF and CDF are respectively given by:

$$F_{\mathrm{IPHL}}(x;\alpha,\beta)=1-\frac{1-e^{-\alpha x^{-\beta}}}{1+e^{-\alpha x^{-\beta}}},\qquad x,\alpha,\beta>0. \tag{3}$$

The corresponding PDF is given by:

$$f_{\mathrm{IPHL}}(x;\alpha,\beta)=\frac{2\alpha\beta x^{-(\beta+1)}e^{\alpha x^{-\beta}}}{\left(1+e^{\alpha x^{-\beta}}\right)^2},\qquad x,\alpha,\beta>0. \tag{4}$$

In these equations, the parameters α and β represent the scale parameter and shape parameter, respectively. The scale parameter α primarily controls the spread or scaling of the distribution, while the shape parameter β governs the overall form or curvature of the distribution.

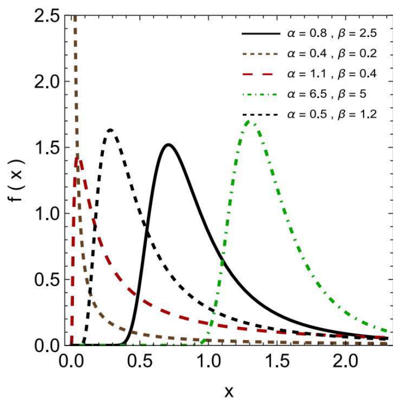

Fig. 1: The PDF of the IPHL distribution for some parameter values.

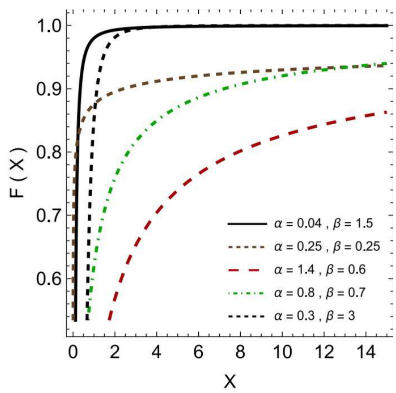

Fig. 2: The CDF of the IPHL distribution for some parameter values.

Figures 1 and 2 display various plots of the distribution's PDF and CDF under different parameter values. The IPHL distribution's PDF demonstrates notable flexibility, assuming a wide range of shapes, which makes it suitable for modeling lifetime data with non-monotone failure rate characteristics as discussed in [23].

In reliability analysis, the survival function represents the probability that a unit survives beyond a specified time. It is typically conducted by evaluating correlations among scores obtained from repeated administrations of the same scale. Consider a lifetime as a continuous random variable characterized by a PDF and CDF, defined over the interval $(0,\infty)$. The reliability function, also known as the survival function, is then formally expressed as in [17]:

$$R(x) = \int_x^{\infty} f(u)\,du.$$

In this study, the reliability function is derived for the IPHL distribution.

$$R_{\text{IPHL}}(x) = 1 - F_{\text{IPHL}}(x) = \frac{1-e^{-\alpha x^{-\beta}}}{1+e^{-\alpha x^{-\beta}}} x > 0. \quad (5)$$

Properties of the survival function:

1.Every survival function $R(t)$ is monotonically decreasing, i.e., $R(u) \leq R(t)$ for all $u > t$.
2.$R(0) = 1$.
3.$R(\infty) = 0$.

The hazard function, also known as the instantaneous failure rate, is defined as the instantaneous rate at which failures occur among units that have survived up to a given time t, within an infinitesimally small subsequent time interval, in populations of non-repairable systems. This measure is expressed as a rate per unit time. Units that have previously failed are excluded from consideration since the hazard function concerns only the surviving units, and its value may change over successive instants of time. The hazard function is commonly denoted by $h(t)$ and was initially introduced by Gross and Clark [21]. According to Nair et al. [33], it can be mathematically expressed as:

$$h(x) = \frac{f(x)}{R(x)}.$$

The hazard function will specifically be applied to the IPHL distribution.

$$h_{\text{IPHL}}(x) = \frac{2\alpha\beta x^{-\beta-1} e^{\alpha x^{-\beta}} \left(1+e^{-\alpha x^{-\beta}}\right)}{\left(1-e^{-\alpha x^{-\beta}}\right)\left(1+e^{\alpha x^{-\beta}}\right)^2}, x > 0. \quad (6)$$

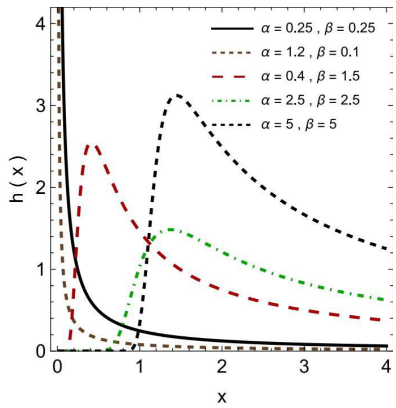

Fig. 3: The hazard function of the IPHL distribution for some parameter values.

Figure 3 shows the hazard function of the IPHL distribution for different values of α and β, highlighting its flexibility in producing decreasing, increasing, and unimodal hazard shapes depending on the parameter values.

The reversed hazard rate function is defined as the ratio of the PDF to the CDF of a random variable. This property provides several important advantages, including the capability to model environmental effects effectively using proportional hazard models. Furthermore, the reversed hazard rate function utilizes the fundamental exponential relationship to uniquely determine the distribution function associated with the time-to-failure random variable. Mathematically, the reversed hazard rate was initially introduced by White [14] and can be expressed as follows:

$$r(x) = \frac{f(x)}{F(x)}, \qquad x > 0.$$

The reversed hazard rate function will specifically be applied to the IPHL distribution.

$$r_{\text{IPHL}}(x) = \frac{\alpha\beta x^{-\beta-1} e^{\alpha x^{-\beta}}}{1+e^{\alpha x^{-\beta}}}, \qquad x > 0. \quad (7)$$

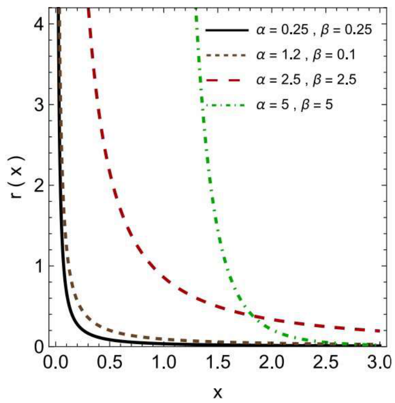

Fig. 4: The reversed hazard function of the IPHL distribution for some parameter values.

Figure 4 shows the reversed hazard function of the IPHL distribution for different values of α and β, illustrating the effect of parameter changes on the decreasing behavior of the reversed hazard rate.

3 Statistical Properties

This section examines the statistical properties of the *IPHL* distribution, such as the quantile function, median, mode, moments, skewness, kurtosis, moment-generating function, and other properties.

3.1 Moments

For a random variable X that follows the *IPHL* distribution, the rth moment provides important insights into the distribution's shape and behavior. It is a key quantity used to describe characteristics such as the mean, variance, and higher-order moments. The rth moment is defined as follows Papoulis and Pillai [34]:

$$\mu_r = E(x^r) = \int_0^\infty x^r 2\alpha\beta x^{-\beta-1} e^{\alpha x^{-\beta}} (1+e^{\alpha x^{-\beta}})^{-2} dx,$$

by using binomial expansion

$$(1+e^{\alpha x^{-\beta}})^{-2} = \sum_{k=0}^{\infty} \binom{-2}{k} e^{\alpha k x^{-\beta}},$$

then

$$E(x^r) = \sum_{k=0}^{\infty} \binom{-2}{k} 2\alpha\beta \int_0^\infty x^{r-\beta-1} e^{\alpha(k+1)x^{-\beta}} dx, \quad (8)$$

let $-y = \alpha(k+1)x^{-\beta}$ in Eq. (8), after simplification, it will take the following form:

$$E(x^r) = \sum_{k=0}^{\infty} \binom{-2}{k} - 2\alpha\beta(-1) \quad (9)$$
$$(\alpha(k+1))^{\frac{r}{\beta}-1} \Gamma(\frac{-r}{\beta}+1).$$

3.2 Moment Generating Function

For a random variable $X \sim IPHL$, both the MGF and the characteristic function (CF) are essential in characterizing the distribution's behavior, especially concerning the sum of random variables and convergence qualities. The definitions of these functions are as follows Baricz and Pogány [12]:

$$M_x(t) = E(e^{tx}) = \int_0^\infty e^{tx} f(x) dx$$
$$= \sum_{r=0}^{\infty} \frac{t^r}{r!} \int_0^\infty x^r f_{IPHL}(x,\alpha,\beta) dx$$
$$= \sum_{r=0}^{\infty} \frac{t^r}{r!} E(x^r)$$
$$= \sum_{r=0}^{\infty}\sum_{k=0}^{\infty} \frac{t^r}{r!} \binom{-2}{k} - 2\alpha\beta(-1)^{1-\frac{r}{\beta}} \quad (10)$$
$$(\alpha(k+1))^{\frac{r}{\beta}-1} \Gamma(\frac{-r}{\beta}+1).$$

By substituting t with it, the characteristic function can be obtained as follows:

$$\varphi_x(t) = \sum_{r=0}^{\infty}\sum_{k=0}^{\infty} \frac{(it)^r}{r!} \binom{-2}{k} - 2\alpha\beta(-1)^{1-\frac{r}{\beta}} \quad (11)$$
$$(\alpha(k+1))^{\frac{r}{\beta}-1} \Gamma(\frac{-r}{\beta}+1).$$

3.3 Quantile and Median

For a random variable $X \sim IPHL(\alpha,\beta)$, the pth quantile, represented as x_p, signifies the value under which the proportion p of the data falls. It is an essential instrument in statistical analyses and assessments of inequality. The pth quantile of the *IPHL* distribution is expressed as Kayid [24]:

$$F(x_p) = p, 0 < p < 1, \quad (12)$$

from Eq. (12), x_p can be obtained as follows

$$x_p = \frac{-1}{\alpha^{\frac{-1}{\beta}}\beta} \ln(\frac{2}{p}-1). \quad (13)$$

Setting $p = 0.5$ in Eq. (13),we get the median of *IPHL* distribution as follows

$$Median = -\ln(3)\frac{\alpha^{\frac{1}{\beta}}}{\beta}. \quad (14)$$

3.4 Mode

The mode of the *IPHL* distribution is determined by differentiating its *PDF* with respect to x and setting the derivative equal to zero.

The mode is subsequently ascertained by resolving the resultant equation:

$$\frac{df_{IPHL}(x,\alpha,\beta)}{dx}=0, \quad (15)$$

By substituting the *PDF* from Eq. (4) into Eq. (15), we obtain

$$2\alpha\beta x^{-2(\beta+1)}e^{\alpha x^{-\beta}}(1+e^{\alpha x^{-\beta}})^{-3} \times\left(\alpha\beta(e^{\alpha x^{-\beta}}-1)-(\beta+1)x^{\beta}(e^{\alpha x^{-\beta}}+1)\right)=0. \quad (16)$$

For (p) uniformly distributed over $(0,1)$, the first, second, and third quartiles of the *IPHL* distribution can be derived by substituting $p=0.25, 0.5$, and 0.75 into Eq. (13). Furthermore, the Bowley's skewness and Moors' kurtosis measures can be computed using the quantile function *QF* as follows:

$$S_k=\frac{Q(3/4)-2Q(1/2)+Q(1/4)}{Q(3/4)-Q(1/4)}, \quad (17)$$

$$K_u=\frac{Q(7/8)-Q(5/8)-Q(1/8)+Q(3/8)}{Q(3/4)-Q(1/4)}, \quad (18)$$

where $Q(.)$ represents the quantile function.

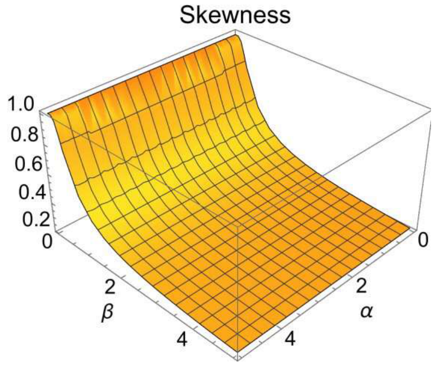

Fig. 5: Skewness Surface of the IPHL Distribution

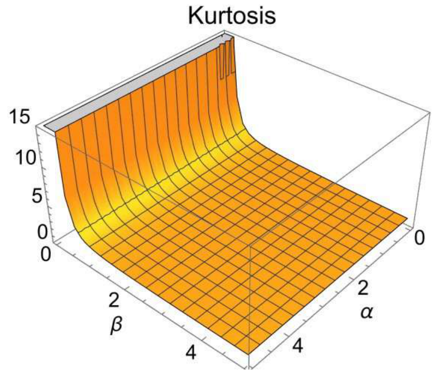

Fig. 6: Kurtosis Surface of the IPHL Distribution

The skewness and kurtosis of the *IPHL* model can be visually represented for selected values of α and β in Figures 5 and 6.

3.5 Order Statistics

Order statistics are extensively utilized in reliability analysis and life testing because of their fundamental importance for statistical inference. Let $X_1, X_2, \ldots\ldots, X_n$ represent a random sample extracted from the *IPHL* distribution. The associated order statistics are represented as $X_{(1)}, X_{(2)}, \ldots\ldots, X_{(n)}$. The *PDF* of the *rth* order statistic is expressed as Khalifa [25]:

$$f_{x(r)}(X)=\frac{f(x)}{\mathbf{B}(r,n-r+1)}\sum_{J=0}^{n-r}(-1)^J\binom{n-r}{J}[F(x)]^{J+r-1},$$

then,

$$f_{x(r)}(X)=\frac{1}{\mathbf{B}(r,n-r+1)}\sum_{J=0}^{n-r}(-1)^J\binom{n-r}{J}(2)^{J+r} \alpha\beta x^{-\beta-1}e^{\alpha x^{-\beta}}(1+e^{\alpha x^{-\beta}})^{-2}(1+e^{\alpha x^{-\beta}})^{-J-r+1},$$

by using binomial expansion

$$(1+e^{\alpha x^{-\beta}})^{-J-r-1}=\sum_{k=0}^{\infty}(-1)^k\binom{J+k+r}{k}e^{\alpha k x^{-\beta}},$$

then

$$f_{x(r)}(X)=\frac{\alpha\beta x^{-1-\beta}}{\mathbf{B}(r,n-r+1)}\sum_{k=0}^{\infty}\sum_{J=0}^{n-r}(-1)^{J+k}(2)^{J+r} \binom{n-r}{J}\binom{J+k+r}{k}e^{\alpha(k+1)x^{-\beta}}. \quad (19)$$

3.6 Mean Residual Life Function

If X follows the $IPHL$ distribution, the MRL function, denoted by $\mu(t)$, gives the expected remaining lifetime conditional on survival up to time t. It serves a crucial role in reliability theory and survival analysis. The MRL function of the $IPHL$ distribution can be expressed as Poynor and Kottas [35]:

$$\mu(t) = \frac{\left[E(t) - \int_0^t x f(x) dx\right] - t}{R(t)}, t \geq 0,$$

therefore,

$$\int_0^t x\, f(x)\, dx = \int_0^t 2\alpha\beta x^{-\beta} \frac{e^{\alpha x^{-\beta}}}{(1+e^{\alpha x^{-\beta}})^2} dx,$$

by using binomial expansion

$$(1+e^{\alpha x^{-\beta}})^{-2} = \sum_{k=0}^{\infty} \binom{-2}{k} e^{\alpha k x^{-\beta}},$$

then

$$\int_0^t x f(x) dx = \sum_{k=0}^{\infty} \binom{-2}{k} e^{\alpha k x^{-\beta}} \int_0^t x^{-\beta} e^{\alpha(k+1)x^{-\beta}} dx. \quad (20)$$

If $-y = \alpha(k+1)x^{-\beta}$ in Eq. (20), after simplification, it will take the following form:

$$\int_0^t x f(x) dx = \sum_{k=0}^{\infty} \binom{-2}{k} 2\alpha(-1)^{\frac{-1}{\beta}} (\alpha(k+1))^{\frac{1}{\beta}-1}$$
$$\Gamma(\frac{-1}{\beta} - 1, -\alpha(k+1)t^{-\beta}), \quad (21)$$

by using Eq. (21) and putting $r = 1$, we obtain

$$E(t) = \sum_{k=0}^{\infty} \binom{-2}{k} - 2\alpha\beta(-1)$$
$$(\alpha(k+1))^{\frac{1}{\beta}-1} \Gamma(\frac{-1}{\beta} + 1),$$

then,

$$\mu(t) = \left(\frac{1-e^{-\alpha t^{-\beta}}}{1+e^{-\alpha t^{-\beta}}}\right)^{-1}$$
$$\times \left(\left[\left(\sum_{k=0}^{\infty} \binom{-2}{k} (-2\alpha\beta)(-1)^{1-\frac{1}{\beta}} (\alpha(k+1))^{\frac{1}{\beta}-1} \Gamma\left(\frac{-1}{\beta}+1\right)\right) \right.\right.$$
$$\left.\left. - \left(\sum_{k=0}^{\infty} \binom{-2}{k} 2\alpha(-1)^{-\frac{1}{\beta}} (\alpha(k+1))^{\frac{1}{\beta}-1} \Gamma\left(\frac{-1}{\beta} - 1, -\alpha(k+1)t^{-\beta}\right)\right)\right] \right.$$
$$\left. - t \right), \qquad t \geq 0. \quad (22)$$

3.7 Rényi Entropy

For a d-dimensional real-valued random vector $X = (X^1; X^2; X^3; ..., X^d)$, with a joint PDF $g : R^d \longrightarrow R$ and marginal densities $g_i : R \longrightarrow R$ for $1 \leqslant i \leqslant d$, the Rényi entropy of order $p \neq 1$ functions as a generalized metric of uncertainty or information content. It broadens the traditional Shannon entropy and is especially advantageous in scenarios necessitating sensitivity to infrequent occurrences. The Rényi entropy of a univariate $IPHL$ random variable X may be articulated in accordance with the general formulation of Rényi entropy and the characteristics of the $IPHL$ distribution Leonenko et al. [27].

$$I_R(x) = \frac{1}{1-R} \ln \left[\int_0^{\infty} f(x)^R dx \right], \ \forall R \neq 1, R > 0,$$
$$= \frac{1}{1-R} \ln \left[(2\alpha\beta)^R \int_0^{\infty} x^{-R(\beta+1)} \frac{e^{\alpha R x^{-\beta}}}{(1+e^{\alpha x^{-\beta}})^{2R}} dx \right], \quad (23)$$

where,

$$(1+e^{\alpha x^{-\beta}})^{-2R} = \sum_{n=0}^{\infty} \binom{-2R}{n} e^{\alpha n x^{-\beta}},$$

let $-y = \alpha(R+n)x^{-\beta}$ in Eq. (23), after simplification, it will take the following form:

$$I_R(x) = \frac{1}{1-R} \ln \left[- \sum_{n=0}^{\infty} \binom{-2R}{n} \right.$$
$$\left. \times \frac{2^R \alpha^R \beta^{R-1} (-1)^{\frac{R}{\beta}(\beta+1)-\frac{1}{\beta}}}{[\alpha(R+n)]^{\frac{R}{\beta}(\beta+1)-\frac{1}{\beta}}} \right]. \quad (24)$$

3.8 Stress-Strength Parameter

The stress-strength reliability measure indicates the probability that the strength X of a system will be greater than the imposed stress Y, denoted as:

$$R = P(Y < X).$$

Assume that $X \sim IPHL(\alpha_1, \beta)$ and $Y \sim IPHL(\alpha_2, \beta)$, where X represents the system's strength and Y represents the applied stress. The stress-strength reliability measure R is then given by:

$$R = \sum_{i=0}^{\infty} \sum_{k=0}^{\infty} \binom{-2}{i} \binom{-1}{k} 4\alpha_1 (\alpha_1(i+1) + \alpha_2 k)^{-1}. \quad (25)$$

Proof.

$$R=\int_0^\infty f_{IPHL}(\alpha_1,\beta)F_{IPHL}(\alpha_2,\beta)dx,$$

then,

$$R=\int_0^\infty 4\alpha_1\beta x^{-\beta-1}e^{\alpha_1 x^{-\beta}}(1+e^{\alpha_1 x^{-\beta}})^{-2}(1+e^{\alpha_2 x^{-\beta}})dx,$$

by using binomial expansion of

$$(1+e^{\alpha_1 x^{-\beta}})^{-2}=\sum_{i=0}^{\infty}\binom{-2}{i}e^{\alpha_1 i x^{-\beta}},$$

and

$$(1+e^{\alpha_2 x^{-\beta}})^{-1}=\sum_{k=0}^{\infty}\binom{-1}{k}e^{\alpha_2 i x^{-\beta}},$$

therefore,

$$R=\sum_{i=0}^{\infty}\sum_{k=0}^{\infty}\binom{-2}{i}\binom{-1}{k}4\alpha_1\beta\int_0^\infty x^{-1-\beta}e^{x^{-\beta}(\alpha_1(i+1)+\alpha_2 k)}dx, \tag{26}$$

let $-y=x^{-\beta}(\alpha_1(i+1)+\alpha_2 k)$ in Eq. (26), after simplification, it will take the following form:

$$R=\sum_{i=0}^{\infty}\sum_{k=0}^{\infty}\binom{-2}{i}\binom{-1}{k}4\alpha_1\frac{1}{(\alpha_1(i+1)+\alpha_2 k)}\int_0^\infty e^{-y}dy.$$

Thus, the computation of this integration

$$\int_0^\infty e^{-y}dy=1.$$

This completes the proof.

4 Method of Estimation

This section provides point and interval estimates for the unknown parameters of the *IPHL* distribution.

4.1 Maximum Likelihood Estimation

Consider a random sample $x_1,x_2,....,x_n$ drawn from the *IPHL* distribution. The likelihood function denotes the joint probability of observing this sample, under the assumption that each observation is independently and identically distributed according to the *IPHL* model. This is the foundation of the estimation of the distribution's unknown parameters. The likelihood function corresponding to the sample is expressed as Millar [30]:

$$L(x;\alpha,\beta)=\prod_{i=1}^{n}(2\alpha\beta)\left(x_i^{-\beta-1}(1+e^{\alpha x_i^{-\beta}})^{-2}\right)e^{\alpha x_i^{-\beta}},$$

and then we take logarithm of $L(\alpha,\beta)$

$$\ell(x,\alpha,\beta)=n\ln(2\alpha\beta)+(-\beta-1)\sum_{i=1}^{n}\ln(x_i)+\sum_{i=1}^{n}\alpha x_i^{-\beta}-2\sum_{i=1}^{n}\ln(1+e^{\alpha x_i^{-\beta}}). \tag{27}$$

By taking the partial derivatives of Eq. (27) with respect to α and β, the *MLE* estimates $\hat{\alpha}$ and $\hat{\beta}$ can be derived by solving the following system of nonlinear equations:

$$\frac{\partial\ell}{\partial\alpha}=\frac{n}{\alpha}+\sum_{i=1}^{n}x_i^{-\beta}-2\sum_{i=1}^{n}x_i^{-\beta}e^{\alpha x_i^{-\beta}}(1+e^{\alpha x_i^{-\beta}})^{-1}=0, \tag{28}$$

$$\frac{\partial\ell}{\partial\beta}=\frac{n}{\beta}-\sum_{i=1}^{n}\alpha x_i^{-\beta}\ln(x_i)-\sum_{i=1}^{n}\ln(x_i)+2\sum_{i=1}^{n}\alpha x_i^{-\beta}\ln(x_i)e^{\alpha x_i^{-\beta}}(1+e^{\alpha x_i^{-\beta}})^{-1}=0. \tag{29}$$

The *MLEs* of parameters α,β are obtained by simultaneously solving nonlinear equations using the Newton-Raphson method. The construction of the asymptotic confidence interval for the *MLEs*, $\hat{\alpha}$ and $\hat{\beta}$, denoted as ACI_{MLE}, is based on the asymptotic normality of the estimators, since closed-form expressions are not available. It is well established that the distribution of the *MLEs* can be approximated by a multivariate normal distribution with mean zero and variance–covariance matrix $I^{-1}(\hat{\alpha},\hat{\beta})$ where $I(\alpha,\beta)$ represents the observed information matrix, defined as follows:

$$I(\alpha,\beta)=\begin{pmatrix}-\frac{\partial^2\ell}{\partial\alpha^2} & -\frac{\partial^2\ell}{\partial\alpha\partial\beta}\\ -\frac{\partial^2\ell}{\partial\beta\partial\alpha} & -\frac{\partial^2\ell}{\partial\beta^2}\end{pmatrix}, \tag{30}$$

where

$$\frac{\partial^2\ell}{\partial\alpha^2}=\frac{-n}{\alpha^2}-2\sum_{i=1}^{n}x_i^{-2\beta}e^{\alpha x_i^{-\beta}}(1+e^{\alpha x_i^{-\beta}})^{-2}, \tag{31}$$

$$\frac{\partial^2\ell}{\partial\beta^2}=\begin{pmatrix}\frac{-n}{\beta^2}-\sum_{i=1}^{n}\alpha x_i^{-\beta}(\ln(x_i))^2+\sum_{i=1}^{n}\alpha e^{\alpha x_i^{-\beta}}\ln^2(x_i)\\ x_i^{-2\beta}(1+e^{\alpha x_i^{-\beta}})^{-2}(x_i^{\beta}e^{\alpha x_i^{-\beta}}+x_i^{\beta}+\alpha)\end{pmatrix}, \tag{32}$$

$$\frac{\partial^2\ell}{\partial\alpha\partial\beta}=\begin{pmatrix}\sum_{i=1}^{n}-x_i^{-\beta}\ln(x_i)+2\sum_{i=1}^{n}x_i^{-2\beta}e^{\alpha x_i^{-\beta}}\ln(x_i)\\ (1+e^{\alpha x_i^{-\beta}})^{-2}(x_i^{\beta}e^{\alpha x_i^{-\beta}}+x_i^{\beta}+\alpha)\end{pmatrix}. \tag{33}$$

Where, the asymptotic $100\%(1-\gamma)$ confidence intervals for $\hat{\alpha}$ and $\hat{\beta}$ are given by

$$\left[\hat{\alpha} \pm z_{1-\frac{\gamma}{2}}\sqrt{var(\hat{\alpha})}, \hat{\beta} \pm z_{1-\frac{\gamma}{2}}\sqrt{var(\hat{\beta})}\right],$$

and, $1-z_{\gamma/2}$ is the quantile from the standard normal distribution corresponding to the desired confidence level.

4.2 Bayesian Estimation

This section presents BE based on the premise that model parameters are random variables. The Bayesian framework is an effective instrument in reliability analysis, facilitating the integration of prior knowledge with observed data analysis. As new data become available, the Bayesian method continuously updates the knowledge about the unknown parameters by treating them as random variables with evolving distributions. For the $IPHL$ distribution, the parameters α and β are assumed to be independent, and each follows a Gamma prior distribution. Bayesian reliability inference has also been widely studied in recent works [18,38].

$$\begin{Bmatrix} \pi_1(\alpha) \propto \alpha^{a_1-1}e^{-b_1\alpha}, \alpha>0, a_1>0, b_1>0 \\ \pi_2(\beta) \propto \beta^{a_2-1}e^{-b_2\beta}, \beta>0, a_2>0, b_2>0, \end{Bmatrix}, \tag{34}$$

where the hyperparameters a_i and b_i, for $(i=1,2)$ are selected to represent previous assumptions when the parameters are unknown. Bayes' theorem is then used to combine the prior distribution with the likelihood function to obtain the joint posterior distribution which can be written as:

$$\begin{aligned}\pi^*(\alpha,\beta|x) &= \frac{\pi_1(\alpha)\pi_2(\beta)L(\alpha,\beta|x)}{\int_0^\infty\int_0^\infty \pi_1(\alpha)\pi_2(\beta)L(\alpha,\beta|x)d\alpha d\beta} \\ &\propto 2^n\alpha^{n+a_1-1}\beta^{n+a_2-1}e^{-b_1\alpha-b_2\beta}\cdot e^{\sum_{i=1}^{n}\alpha x_i^{-\beta}} \\ &\quad \prod_{i=1}^{n} x_i^{-\beta-1}(1+e^{\alpha x_i^{-\beta}})^{-2}.\end{aligned} \tag{35}$$

The marginal conditional distributions for α and β are derived as follows:

$$\pi^*(\alpha|\beta,x) \propto \alpha^{n+a_1-1}e^{-b_1\alpha+\sum_{i=1}^{n}\alpha x_i^{-\beta}}\prod_{i=1}^{n}(1+e^{\alpha x_i^{-\beta}})^{-2}, \tag{36}$$

$$\begin{aligned}\pi^*(\beta|\alpha,x) &\propto \beta^{n+a_2-1}e^{-b_2\beta+\sum_{i=1}^{n}\alpha x_i^{-\beta}} \\ &\quad\times\prod_{i=1}^{n} x_i^{-\beta-1}(1+e^{\alpha x_i^{-\beta}})^{-2}.\end{aligned} \tag{37}$$

In Bayesian analysis, the squared error loss (SEL) function is employed for its simplicity and equal treatment of over- and underestimation, yielding posterior means as Bayes estimators. Since the conditional posteriors of α and β are not analytically tractable, the Metropolis–Hastings $(M-H)$ algorithm within the $MCMC$ framework is applied to generate posterior samples, enabling estimation and credible interval construction.

Steps of the $M-H$ Algorithm

1. Begin by selecting initial values for the model parameters, denoted as (α^0, β^0)
2. Initialize the iteration index with $j=1$
3. Iterate the $M-H$ sampling process, generate new values for α^j, β^j using their conditional posterior distributions:

$$\hat{\pi}_1^*(\alpha^{j-1}|\beta^{j-1},x)$$
$$\hat{\pi}_2^*(\beta^{j-1}|\alpha^{j-1},x).$$

These distributions are typically normal:

$$N(\alpha^{j-1}, var(\alpha)), N(\beta^{j-1}, var(\beta)).$$

4. Propose new values by drawing candidate values from the proposal distributions using the Metropolis sampling approach described by Martino and Elvira [29]:

$$\grave{\alpha} \sim N(\alpha^{j-1}, var(\alpha^{j-1})),$$
$$\grave{\beta} \sim N(\beta^{j-1}, var(\beta^{j-1})).$$

5. Compute acceptance probabilities

$$\eta_\alpha = \min(1, \frac{\hat{\pi}_1^*(\grave{\alpha}|\beta^{j-1},x)}{\hat{\pi}_1^*(\alpha^{j-1}|\beta^{j-1},x)}),$$

$$\eta_\beta = \min(1, \frac{\hat{\pi}_2^*(\grave{\beta}|\alpha^{j-1},x)}{\hat{\pi}_2^*(\beta^{j-1}|\alpha^{j-1},x)}).$$

6. Generate uniform random values sample $u_1, u_2 \sim U(0,1)$.
7. Accept or reject proposed values:
a. if $u_1 < \eta_\alpha$ accept $\alpha^j = \grave{\alpha}$, otherwise set $\alpha^j = \alpha^{j-1}$
b. if $u_2 < \eta_\beta$ accept $\beta^j = \grave{\beta}$, otherwise set $\beta^j = \beta^{j-1}$
8. Update the iteration index by setting: $j = j+1$.
9. Continue steps 3 through 8 for a total of N iterations, as defined by the study design
10. Compute the Bayesian estimates under the SEL function as follows: $\hat{\alpha}_{BE} = \frac{1}{K-K_0}\sum_{j=K_0+1}^{K}\alpha^j$ and $\hat{\beta}_{BE} = \frac{1}{K-K_0}\sum_{j=K_0+1}^{K}\beta^j$,

here, K_0 is the number of burn-in iterations discarded to reduce the effect of initial parameter values.

11. Construct $100(1-\gamma)\%$ Bayesian credible intervals ($CRIs$) for the parameter estimates by computing the $\frac{\gamma}{2}$ and $1-\frac{\gamma}{2}$ quantiles of the empirical posterior distribution derived from the $MCMC$ samples.

4.3 Maximum Product Spacing Estimator

The MPS method, introduced by Cheng and Amin [15] Further discussions on the MPS approach can be found in [8,20] and further discussed by Anatolyev and Kosenok [8], is a robust alternative to traditional likelihood-based estimation techniques. This approach is based on the assumption that the spacings – defined as the differences between successive CDF values−should follow a uniform pattern across the ordered data points. Consider an ordered sample $x_{(1)},x_{(2)},\ldots,x_{(n)}$ of size n from $IPHL$ distribution. The spacing at the $i-th$ observation is defined as follows:

$$D_i(\alpha,\beta)=\int_{x_{(i-1)}}^{x_{(i)}} f(x;\alpha,\beta)dx; i=1,2,\ldots,n+1, \quad (38)$$

where $F(x_{(0)};\alpha,\beta)=0$ and $F(x_{(n+1)};\alpha,\beta)=1$. The geometric mean of the differences can be expressed as:

$$G(\alpha,\beta)=(\prod_{i=1}^{n+1} D_i(\alpha,\beta))^{\frac{1}{n+1}}. \quad (39)$$

By maximizing the logarithm of the geometric mean of spacings and substituting Eq. (3) into Eq. (40), we obtain:

$$\ln G=\frac{1}{n+1}\sum_{i=1}^{n+1}\ln(F(x_{(i)};\alpha,\beta)-F(x_{(i-1)};\alpha,\beta)), \quad (40)$$

by solving the following nonlinear equations simultaneously, the MPS estimation ($\hat{\alpha}^*_{MPS}$) and ($\hat{\beta}^*_{MPS}$) of α and β are found:

$$\frac{d\ln G}{d\alpha}=\frac{1}{n+1}\sum_{i=1}^{n+1}\frac{\acute{F}_\alpha(x_{(i)};\alpha,\beta)-\acute{F}_\alpha(x_{(i-1)};\alpha,\beta)}{F(x_{(i)};\alpha,\beta)-F(x_{(i-1)};\alpha,\beta)}=0, \quad (41)$$

and

$$\frac{d\ln G}{d\beta}=\frac{1}{n+1}\sum_{i=1}^{n+1}\frac{\acute{F}_\beta(x_{(i)};\alpha,\beta)-\acute{F}_\beta(x_{(i-1)};\alpha,\beta)}{F(x_{(i)};\alpha,\beta)-F(x_{(i-1)};\alpha,\beta)}=0, \quad (42)$$

where $\acute{F}_\alpha(x;\alpha,\beta)=-\frac{2x^{-\beta}e^{\alpha x^{-\beta}}}{(1+e^{\alpha x^{-\beta}})^2}$ and $\acute{F}_\beta(x;\alpha,\beta)=\frac{2\alpha\ln(x)x^{-\beta}e^{\alpha x^{-\beta}}}{(1+e^{\alpha x^{-\beta}})^2}$

The asymptotic confidence intervals for the parameters α and β, obtained via the MPS estimation method, are based on the well-established asymptotic equivalence between the MLE and MPS approaches, as discussed by Poynor and Kottas [35], Sharma et al. [37], and Yu et al. [39]. Accordingly, the $100(1-\gamma)\%$ asymptotic confidence intervals for the parameters using MPS are expressed as follows:

$$\hat{\alpha}_{MPS}\pm z_{1-\frac{\gamma}{2}}\sqrt{var(\hat{\alpha}_{MPS})} \text{ and } \hat{\beta}_{MPS}\pm z_{1-\frac{\gamma}{2}}\sqrt{var(\hat{\beta}_{MPS})},$$

where $\hat{\alpha}_{MPS}$ and $\hat{\beta}_{MPS}$ are the MPS estimators of the parameters α and β, respectively. The term $z_{1-\frac{\gamma}{2}}$ denotes the critical value from the standard normal distribution, and $var(\hat{\alpha}_{MPS})$ $var(\hat{\beta}_{MPS})$, represent the asymptotic variances, computed using the inverse of the observed information matrix, as given in Eq. (30).

4.4 Least Squares Estimation

The LSE method offers a practical approach to estimating unknown parameters by minimizing the sum of squared differences between the theoretical CDF of the $IPHL$ distribution and the empirical CDF derived from the sample. Consider an ordered sample $x_{(1)},x_{(2)},\ldots,x_{(n)}$ of size n from $IPHL$ distribution.

To obtain the LSE for the parameters α and β, the following objective function is minimized:

$$SS=\sum_{i=1}^{n}(F(x_{(i)},\alpha,\beta)-E(F(x_{(i)},\alpha,\beta))^2,$$

with respect to α and β, where $E(F(x_{(i)},\alpha,\beta))=\frac{i}{(n+1)}$ for $i=1,2,\ldots..,n$. Then $\hat{\alpha}_{LSE}$ and $\hat{\beta}_{LSE}$ are solutions of the following equations:

$$\frac{\partial SS}{\partial\alpha}=2\sum_{i=1}^{n}\acute{F}_\alpha(x_{(i)},\alpha,\beta)(F(x_{(i)},\alpha,\beta)-\frac{i}{(n+1)})=0,$$
$$\frac{\partial SS}{\partial\beta}=2\sum_{i=1}^{n}\acute{F}_\beta(x_{(i)},\alpha,\beta)(F(x_{(i)},\alpha,\beta)-\frac{i}{(n+1)})=0.$$

where $\acute{F}_\alpha(x;\alpha,\beta)$ and $\acute{F}_\beta(x;\alpha,\beta)$ are defined in Eqs. (41) and (42).

4.5 Bootstrap Confidence Intervals

Bootstrap confidence intervals provide a non-parametric method for quantifying the uncertainty surrounding sample statistics–such as the mean, variance, or median–without relying on specific assumptions regarding the underlying population distribution.

Boot-p Method

1. Calculate the LSE estimators: $\hat{\alpha}_{LSE}$ and $\hat{\beta}_{LSE}$ for the $IPHL$ distribution.

2.Generate a bootstrap sample using these estimates and compute new estimates: $(\hat{\alpha}_b, \hat{\beta}_b)$.
3.Repeat the process $N-$times to get N sets of estimates: $(\hat{\alpha}_{b_1}, \hat{\beta}_{b_1}), (\hat{\alpha}_{b_2}, \hat{\beta}_{b_2}), ..., (\hat{\alpha}_{b_N}, \hat{\beta}_{b_N})$.
4.Construct $100(1-\gamma)\%$ confidence intervals using the empirical distribution of the bootstrap estimates, by taking the $\frac{\gamma}{2}$ and $(1-\frac{\gamma}{2})$ percentiles.

Boot-t Method

Points one through three, as outlined in the Boot-p steps.
4.For each bootstrap sample, the estimates α, β are obtained, and the asymptotic standard errors $SE(\hat{\alpha})$, $SE(\hat{\beta})$ are estimated using the observed Fisher information matrix.
5.Studentized statistics are calculated as follows: $\hat{T}_\alpha = \frac{\hat{\alpha}-\alpha}{SE(\hat{\alpha})}, \alpha \in \{\alpha, \beta\}$.
6.The empirical distribution of $\hat{T}_\alpha$ is used to compute the $\frac{\gamma}{2}$ and $1-\frac{\gamma}{2}$ quantiles, denoted by $t_{\frac{\gamma}{2}}$ and $t_{1-\frac{\gamma}{2}}$,respectively.
7.The two sided $100(1-\gamma)\%$ C.I for $\hat{\alpha}$ is given by:

$$\left[\hat{\alpha} - t_{1-\frac{\gamma}{2}} SE(\alpha), \hat{\alpha} - t_{\frac{\gamma}{2}} SE(\alpha)\right].$$

5 Simulation Study

A simulation study was conducted to assess the efficacy of several estimating approaches for the parameters of the newly introduced $IPHL$ distribution. The aim was to evaluate the precision of four traditional estimation methods: MLE, MPS, LSE, and BE. Random samples were generated from the $IPHL$ distribution using the inverse transformation method. In each simulated scenario, the parameters α and β were assigned fixed values, and the estimators were assessed across five sample sizes: $n = 25$, 50, 100, 150, and 200. Each experiment was repeated 1000 times to ensure statistical stability. Three parameter configurations were examined: ($\alpha = 0.25$, $\beta = 0.25$), ($\alpha = 1.25$, $\beta = 0.75$), and ($\alpha = 2$, $\beta = 2$), to cover a range of distributional shapes. In each run, 1000 bootstrap samples were generated, and $10,000$ $MCMC$ observations were obtained. To reduce the effect of the initial values, the first 1,000 observations were discarded as burn-in, and every third observation was retained through thinning to decrease dependence. The efficacy of the point estimators derived from each approach was evaluated using two conventional accuracy metrics: the Mean Squared Error (MSE) and the Absolute Bias (AB). In addition to point estimates, interval estimates were also considered. Confidence intervals were established using asymptotic methods derived from the MLE and MPS, in addition to two nonparametric bootstrap techniques: the percentile bootstrap$-p$ and the bootstrap$-t$ methods, coupled with (CrI). The intervals were assessed based on their average width (AW) and coverage Probability (CP). Similar simulation-based evaluation procedures were considered by Ramos et al. [36]. yielding a thorough comprehension of their efficacy and dependability. The outcomes are shown in two sets of tables according to each parameter configuration.

Based on the simulation tables, the following findings were obtained:

–The MSE values of all estimators decrease as the sample size increases in all investigated cases.
–The AB tends to approach zero as the sample size increases for all estimation methods.
–The AW of the CIs decreases as the sample size increases for all estimation techniques.
–The AB for the MPS method is predominantly negative.
–Among all compared methods, BE demonstrates the best performance with respect to both MSE and AB.
–The MSE and AB of the LSE estimates are higher than those of the other estimation approaches across all scenarios considered in the simulation.

6 Application

In this section, the proposed $IPHL$ distribution is compared with four other two-parameter distributions: the Generalized Inverted Exponential (GIE) distribution [1], the Inverted Exponentiated Half Logistic $(IEHL)$ distribution [39], the Inverse Gompertz (IGo) distribution [16], and the Inverted Gamma (IG) distribution [28].

To assess and compare the fitted distributions, we employ various goodness-of-fit measures. These include the Kolmogorov–Smirnov distance (KS) with corresponding p-value, the Akaike Information Criterion (AIC), the Bayesian Information Criterion (BIC),the corrected Akaike Information Criterion $(AICC)$, the consistent Akaike Information Criterion $(CAIC)$, the negative log-likelihood $(-Loglik)$, the Anderson–Darling statistic (A^*), and the Cramér–von Mises statistic (W^*).

Parameter estimation for the $IPHL$ distribution was carried out for its shape parameters (α, β) using four estimation methods: MLE, BE, MPS, and LSE. To quantify the uncertainty of the parameter estimates, various types of confidence and credible intervals were constructed, including asymptotic confidence intervals (ACI) derived from MLE and MPS, bootstrap-based intervals (percentile and t-based), and $CrIs$. A comprehensive analysis of the numerical results and their interpretations is provided in a subsequent section.

6.1 Data Set I

The dataset below includes the alleviation periods, measured in hours, documented for a cohort of eighteen patients who received analgesic therapy. This dataset

Table 1: Simulation results for the point estimators when $\alpha = 0.25$ and $\beta = 0.25$.

Parameter	n	MLE		MPS		LSE		BE	
		MSE	AB	MSE	AB	MSE	AB	MSE	AB
α	25	0.0075	0.0092	0.0123	0.0614	0.0113	0.0346	0.0081	0.01
	50	0.0049	0.0034	0.0069	0.0412	0.0063	0.0255	0.0042	0.0118
	100	0.0024	0.0034	0.003	0.0221	0.0033	0.0096	0.0026	-0.0047
	150	0.0019	-0.0023	0.0021	0.0114	0.0021	0.0023	0.0016	0.0031
	200	0.0014	-0.0002	0.0015	0.0107	0.0017	0.0032	0.0009	-0.0013
β	25	0.0016	0.0071	0.0017	-0.0223	0.0025	-0.0057	0.0019	0.0083
	50	0.0009	0.0026	0.001	-0.0151	0.0011	-0.0063	0.0007	0.003
	100	0.0005	0.0018	0.0005	-0.0088	0.0007	-0.0012	0.0005	0.0049
	150	0.0003	0.0039	0.0003	-0.004	0.0004	0.0012	0.0003	0.0019
	200	0.0003	0.0023	0.0003	-0.004	0.0004	0.0006	0.0002	0.0032

Table 2: Simulation results for the interval estimators when $\alpha = 0.25$ and $\beta = 0.25$.

Parameter	n	ACI_{MLE}		ACI_{MPS}		Boot-p		Boot-t		CrI	
		AW	CP	AW	CP	AW	CP	AW	CP	AW	CP
α	25	0.3889	1.02	0.388	0.956	0.3566	0.992	0.3834	0.94	0.3676	0.9512
	50	0.2767	1.008	0.2754	0.94	0.2609	0.992	0.2731	0.96	0.2689	0.9675
	100	0.1934	0.948	0.1928	0.956	0.1847	0.988	0.1894	0.936	0.1786	0.8943
	150	0.1558	0.936	0.1555	0.94	0.1498	0.964	0.1522	0.912	0.1482	0.9024
	200	0.1358	0.948	0.1355	0.928	0.1319	0.968	0.1331	0.948	0.1219	0.9756
β	25	0.1675	1.06	0.1398	0.892	0.1645	0.992	0.164	0.94	0.1596	0.9512
	50	0.116	0.996	0.1037	0.88	0.1135	0.98	0.115	0.94	0.1596	0.9675
	100	0.0815	0.968	0.0761	0.868	0.0798	0.984	0.0803	0.928	0.0778	0.9431
	150	0.0671	0.968	0.0638	0.916	0.0656	0.964	0.0661	0.952	0.0619	0.9024
	200	0.0577	0.924	0.0554	0.92	0.0575	0.94	0.0575	0.916	0.0531	0.935

Table 3: Simulation results for the point estimators when $\alpha = 1.25$ and $\beta = 0.75$.

Parameter	n	MLE		MPS		LSE		BE	
		MSE	AB	MSE	AB	MSE	AB	MSE	AB
α	25	0.0549	0.016	0.044	0.0235	0.0543	0.0132	0.0464	-0.0024
	50	0.0327	0.0179	0.0289	0.0239	0.0321	0.0197	0.0213	-0.0089
	100	0.0126	0.0111	0.0119	0.0165	0.0131	0.0119	0.0141	-0.0056
	150	0.0098	-0.0037	0.0093	0.001	0.0104	-0.0025	0.0104	-0.0056
	200	0.0083	-0.0015	0.0079	0.0025	0.0089	-0.0002	0.006	0.0036
β	25	0.0256	0.0521	0.0194	-0.0396	0.0295	0.0006	0.0245	0.0494
	50	0.0094	0.0183	0.0091	-0.0351	0.0118	-0.0068	0.0085	0.0181
	100	0.0036	0.0086	0.0038	-0.0236	0.0056	-0.0012	0.0033	0.0092
	150	0.003	0.0116	0.0028	-0.012	0.0042	0.0048	0.0026	0.0047
	200	0.0018	0.0071	0.0019	-0.0118	0.0027	0.0019	0.0006	0.0067

Table 4: Simulation results for the interval estimators when $\alpha = 1.25$ and $\beta = 0.75$.

Parameter	n	ACI_{MLE}		ACI_{MPS}		Boot-p		Boot-t		CrI	
		AW	CP	AW	CP	AW	CP	AW	CP	AW	CP
α	25	0.9438	0.944	0.9061	0.96	0.9664	0.968	0.9279	0.94	0.8696	0.9512
	50	0.6671	0.936	0.6505	0.94	0.6745	0.948	0.6608	0.924	0.6299	0.9675
	100	0.4691	0.964	0.4622	0.964	0.4698	0.952	0.4653	0.952	0.4563	0.9431
	150	0.3803	0.94	0.3763	0.94	0.3812	0.936	0.3787	0.94	0.3765	0.9106
	200	0.3296	0.932	0.3269	0.932	0.3286	0.916	0.3269	0.916	0.2792	0.9431
β	25	0.5246	0.944	0.4743	0.852	0.5652	0.932	0.5119	0.86	0.5016	0.9024
	50	0.3521	0.936	0.3323	0.896	0.3622	0.92	0.3499	0.904	0.3408	0.9594
	100	0.2452	0.948	0.2369	0.924	0.2463	0.936	0.2429	0.936	0.2427	0.9594
	150	0.201	0.956	0.196	0.92	0.2006	0.944	0.2	0.948	0.1967	0.9512
	200	0.173	0.952	0.1695	0.924	0.1735	0.952	0.1724	0.952	0.0197	0.9187

Table 5: Simulation results for the point estimators when $\alpha = 2$ and $\beta = 2$.

Parameter	n	MLE		MPS		LSE		BE	
		MSE	AB	MSE	AB	MSE	AB	MSE	AB
α	25	0.1419	0.0693	0.0976	-0.0335	0.1368	0.0151	0.0845	0.0421
	50	0.0656	0.0473	0.0516	-0.0102	0.0737	0.0191	0.0516	0.0234
	100	0.0293	0.03	0.0252	-0.0016	0.0341	0.0137	0.0209	-0.0088
	150	0.02	0.018	0.0182	-0.0041	0.0203	0.0085	0.0171	0.0173
	200	0.0148	0.0048	0.014	-0.0124	0.017	-0.0009	0.0138	0.0201
β	25	0.167	0.1159	0.1382	-0.1268	0.1943	-0.0026	0.1007	0.064
	50	0.0568	0.0422	0.0577	-0.1022	0.0817	-0.0075	0.0644	0.0487
	100	0.0327	0.0214	0.0338	-0.0634	0.0439	-0.0164	0.0336	0.0421
	150	0.0174	0.023	0.0173	-0.0394	0.0234	0.0008	0.0153	0.0147
	200	0.0144	0.025	0.0138	-0.0255	0.0202	0.0144	0.0133	0.0125

Table 6: Simulation results for the interval estimators when $\alpha = 2$ and $\beta = 2$.

Parameter	n	ACI_{MLE}		ACI_{MPS}		Boot-p		Boot-t		CrI	
		AW	CP	AW	CP	AW	CP	AW	CP	AW	CP
α	25	1.3788	0.964	1.2966	0.956	1.5641	0.944	1.3546	0.888	1.2401	0.9512
	50	0.9568	0.936	0.9244	0.952	1.0016	0.916	0.9525	0.908	0.9034	0.9594
	100	0.669	0.952	0.6561	0.964	0.6769	0.932	0.6626	0.928	0.6467	0.9675
	150	0.5429	0.956	0.5354	0.96	0.5476	0.948	0.5404	0.932	0.5247	0.9594
	200	0.4668	0.952	0.4617	0.956	0.4711	0.932	0.4659	0.94	0.445	0.9675
β	25	1.3786	0.948	1.254	0.872	1.4957	0.884	1.3451	0.864	1.258	0.9594
	50	0.9391	0.964	0.8883	0.908	0.9509	0.948	0.9301	0.936	0.908	0.9268
	100	0.6551	0.96	0.6344	0.868	0.6584	0.944	0.6476	0.94	0.6529	0.9512
	150	0.5345	0.96	0.5222	0.936	0.5357	0.936	0.5334	0.944	0.5253	0.9594
	200	0.463	0.964	0.4545	0.932	0.4683	0.948	0.4618	0.948	0.4853	0.9564

was first presented by Gross & Clark [22]. It represents a typical example of real-world time-to-event data commonly observed in healthcare applications.

Table 7: Relief time data for eighteen patients.

1.1	1.2	1.3	1.4	1.4	1.5	1.6	1.7	1.7
1.7	1.8	1.9	2.0	2.2	2.3	2.7	3.0	4.1

According to Table 8,the $IPHL$ distribution exhibited the minimal values for $AIC, BIC, AICC, CAIC$, A^*, and W^* statistics in comparison to the other potential models. Furthermore, it achieved the largest $p-value$ in the $K-S$ test, indicating an exceptional fit to the actual data. The results indicate that the $IPHL$ distribution offers the most optimal alignment among the evaluated models. Figure 7 displays the estimated survival functions and $PDFs$ of the competing distributions fitted to the data set I, visually confirming the advantage of the $IPHL$ distribution in capturing the underlying pattern of the observed data.

Table 9 presents the estimated values of the parameters α and β for the $IPHL$ distribution derived from many estimating techniques, including MLE, BE, MPS, and LSE. It also encompasses interval estimations such as ACI, bootstrap intervals, and asymptotic $CrIs$. These findings provide a comparative analysis of the accuracy and reliability of each estimating technique applied to the relief time data.

Figure 8 demonstrates a smooth and well-behaved histogram for the marginal posterior density, a trace plot where each chain appears to wander around the same region without noticeable trends, and the results from the first 100 lags of the autocorrelation function (ACF). These findings indicate fast convergence of the $MCMC$ chain.

6.2 Data Set II

This study utilizes a dataset of real-world observations about radiation exposure, gathered within the framework of biomedical research. It specifically denotes time-to-event data, quantifying the length (usually in hours) before a particular radiation-related consequence manifests or subsides. The data are continuous and non-negative, making them particularly appropriate for survival and reliability research. These datasets are extensively used in actuarial science, reliability engineering, and medical radiation research, offering significant insights into the applicability and resilience of sophisticated statistical models Alghamdi et al. [3].

According to Table 11, the $IPHL$ distribution exhibited the minimal values for $AIC, BIC, AICC, CAIC$, A^* and W^* statistics in comparison to the other potential models. Furthermore, it achieved the largest $p-value$ in the $K-S$ test, indicating an exceptional fit to the actual data. The results indicate that the $IPHL$ distribution offers the most optimal alignment among the evaluated models. Figure 9 displays the estimated survival and density functions of the competing distributions fitted to the dataset, visually confirming the advantage of the $IPHL$ distribution in capturing the underlying pattern of the observed data.

Table 12 presents the estimated values of the parameters α and β for the $IPHL$ distribution derived from many estimating techniques, including MLE, BE, MPS, and LSE. It also encompasses interval estimations such as ACI, bootstrap intervals, and $CrIs$. These findings provide a comparative analysis of the accuracy and reliability of each estimating technique applied to the radiation exposure data.

Figure 10 demonstrates a smooth and well-behaved histogram for the marginal posterior density, a trace plot where each chain appears to wander around the same region without noticeable trends, and the results from the first 100 lags of the ACF. These findings indicate fast convergence of the $MCMC$ chain.

7 Conclusion

This paper introduced a new flexible lifetime model, termed the $IPHL$ distribution, constructed through an inverse power transformation of the power half-logistic distribution. Several statistical and reliability properties of the proposed model were derived, demonstrating its ability to accommodate a wide range of hazard rate shapes, including increasing, decreasing, unimodal, and bathtub-shaped behaviours. Multiple classical and BE methods were developed and examined, and their performance was systematically evaluated using an extensive Monte Carlo simulation study. The simulation results indicated that the proposed estimators are consistent and that their accuracy improves as the sample size increases, with BE generally exhibiting superior performance.

The practical applicability of the $IPHL$ distribution was illustrated using two real lifetime datasets and compared with several well-known inverse lifetime models. Based on standard goodness-of-fit criteria such as AIC proposed by Akaike [2], and graphical analyses, the $IPHL$ distribution consistently provided a better fit to the data than the competing models. These findings confirm that the proposed distribution offers enhanced flexibility and strong empirical performance, making it a valuable and competitive alternative for modeling complex lifetime and reliability data.

Future research may extend the $IPHL$ model to censored data schemes, multivariate frameworks, and regression structures, with further applications in engineering reliability and biomedical survival analysis.

Table 8: Statistical comparison of fitted distributions for Data Set I.

Model	AIC	BIC	AICC	$-\log L$	W^*	A^*	CAIC	P-value	K–S
$IPHL(\alpha,\beta)$	34.9755	36.9670	35.6814	15.4878	0.0282593	0.168016	35.6814	0.972307	0.108628
$IEHL(\alpha,\beta)$	37.8984	39.8899	38.6043	16.9492	0.0733365	0.440056	38.6043	0.766756	0.148932
$GIE(\alpha,\beta)$	38.2091	40.2006	38.9150	17.1046	0.0805432	0.479178	38.9150	0.728256	0.154228
$IGo(\alpha,\beta)$	36.7830	38.7745	37.4889	16.3915	0.0540297	0.336948	37.4889	0.819806	0.141242
$IG(\alpha,\beta)$	36.0929	38.0843	36.7987	16.0464	0.0474076	0.282721	36.7987	0.876049	0.132138

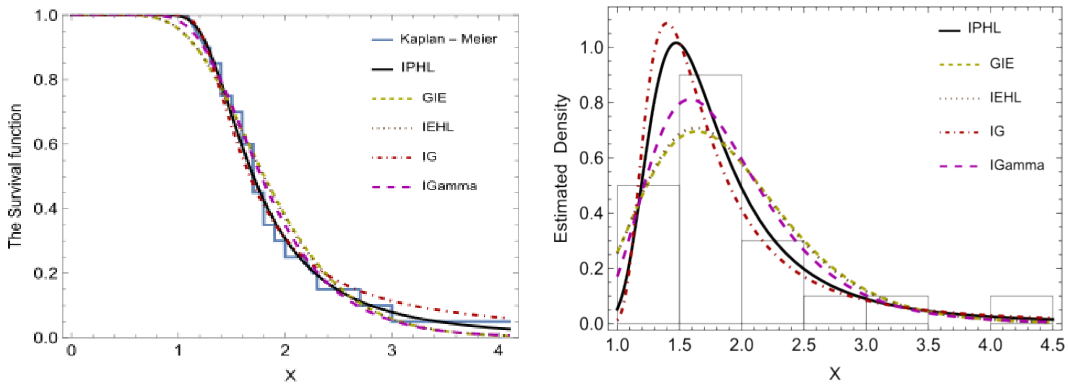

Fig. 7: Estimated survival functions and density functions for Data Set I.

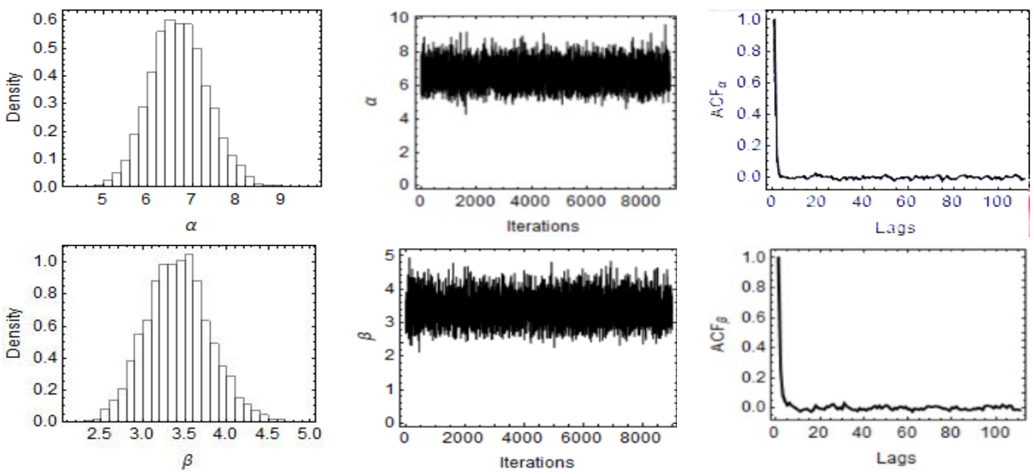

Fig. 8: The histogram of the marginal posterior density, the trace plot, and the autocorrelation values for the first lags based on the MCMC results from Data Set I.

References

[1] A. M. Abouammoh and A. M. Alshingiti. Reliability estimation of generalized inverted exponential distribution. *J. Stat. Comput. Simul.*, 79, 1301–1315 (2009).

[2] H. Akaike. A new look at the statistical model identification. *IEEE Trans. Autom. Control*, 19, 716–723 (1974).

[3] S. M. Alghamdi, I. Elbatal and A. S. Al-Moisheer. Heavy tailed log-Kumaraswamy distribution with modeling to insurance and radiation data sets. *J. Radiat. Res. Appl. Sci.*, 18, 101487 (2025).

[4] H. S. Al-Kzzaz and M. M. E. Abd El-Monsef. Inverse power Maxwell distribution: Statistical properties, estimation and application. *J. Appl. Stat.*, 49, 2287–2306 (2022).

[5] S. Al-Marzouki, F. Jamal, C. Chesneau and M. Elgarhy. Half logistic inverse Lomax distribution with applications. *Symmetry*, 13, 309 (2021).

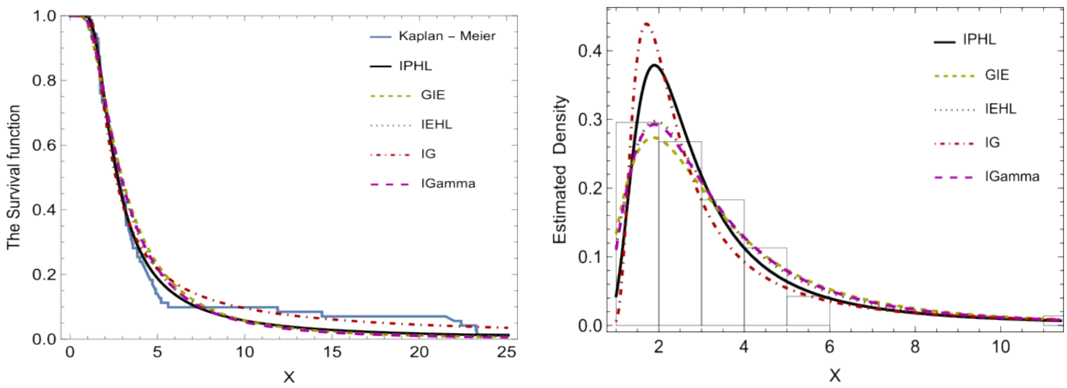

Fig. 9: Estimated survival functions and density functions for Data Set II.

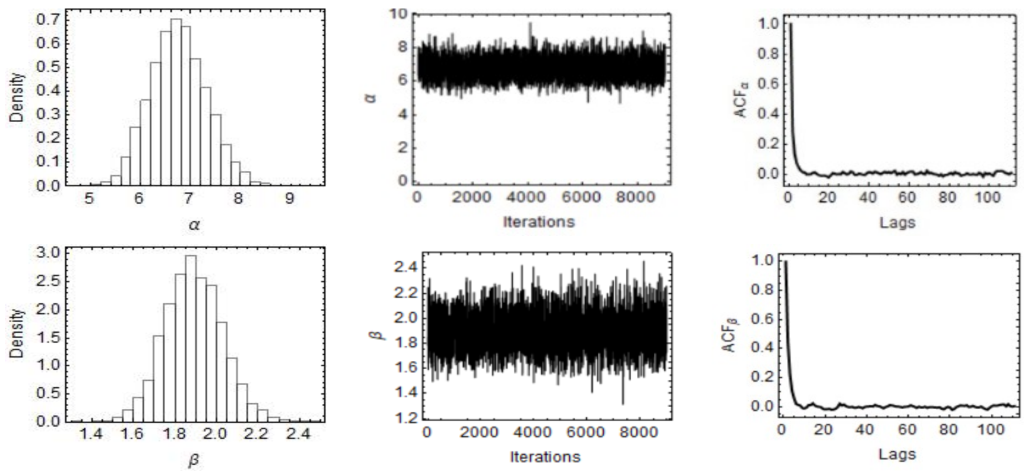

Fig. 10: The histogram of the marginal posterior density, the trace plot, and the autocorrelation values for the first 100 lags based on the MCMC results from Data Set II.

Table 9: Estimated parameters α and β using different methods for Data Set I.

Method	α	β
MLE	6.7771	3.4179
BE	6.7083	3.4193
MPS	5.3853	2.9409
LSE	6.5526	3.3151
ACI_{MLE}	(3.0798, 10.4745)	(2.2043, 4.6315)
CrI	(5.4782, 8.0363)	(2.7050, 4.2139)
ACI_{MPS}	(2.6859, 8.0847)	(1.8861, 3.9958)
Boot-p	(4.6910, 13.7083)	(2.5338, 5.6436)
Boot-t	(5.2575, 11.8262)	(2.7179, 5.1801)

Table 10: Radiation exposure time-to-event data.

1.1219	1.7317	2.5279	3.5942	4.8280
1.2416	1.7374	2.8037	3.2088	4.5295
1.2423	1.8321	2.5859	3.0771	5.2096
1.2429	1.8373	2.3023	3.1806	5.6154
1.5154	1.9648	2.9742	3.8477	5.0801
1.6076	1.9697	2.1174	3.1769	11.8841
1.6273	2.1031	2.1505	3.5619	14.4261
1.6285	2.7093	2.4838	3.8613	21.5954
1.7025	2.4576	2.3952	4.2963	22.3958
1.7046	2.3530	2.7092	4.3917	23.2890
1.7048	2.3961	3.3535	4.4289	23.2415
1.7057	2.2011	3.3790	4.0055	25.0818
1.7111	2.7320	3.4844	4.7198	
1.7289	2.8428	3.2065	4.9065	

[6] M. M. Al Sobhi. The inverse-power logistic-exponential distribution: Properties, estimation methods, and application to insurance data. *Mathematics*, 8, 2060 (2020).

Table 11: Statistical comparison of fitted distributions for Data Set II.

Model	AIC	BIC	AICC	$-\log L$	W^*	A^*	CAIC	P-value	K–S
$IPHL(\alpha,\beta)$	294.970	299.495	295.146	145.485	0.0570	0.6200	295.146	0.8721	0.0705
$IEHL(\alpha,\beta)$	301.919	306.445	302.096	148.960	0.1547	1.2590	302.096	0.6437	0.0878
$GIE(\alpha,\beta)$	306.834	311.359	307.010	151.417	0.2467	1.8264	307.010	0.3616	0.1096
$IGo(\alpha,\beta)$	295.729	300.254	295.905	145.864	0.1014	0.7221	295.905	0.5517	0.0944
$IG(\alpha,\beta)$	303.893	308.418	304.070	149.947	0.1859	1.5159	304.070	0.5252	0.0963

Table 12: Estimated parameters α and β using different methods for Data Set II.

Method	α	β
MLE	6.2080	1.7333
BE	6.7616	1.8920
MPS	5.7497	1.6452
LSE	6.1996	1.7573
ACI_{MLE}	(4.4407, 7.9753)	(1.3966, 2.0699)
CrI	(5.7074, 7.9214)	(1.6299, 2.1696)
ACI_{MPS}	(4.1628, 7.3367)	(1.3253, 1.9651)
Boot-p	(5.0837, 8.6906)	(1.4706, 2.0684)
Boot-t	(5.0528, 8.7589)	(1.4365, 2.1119)

[7] Awajan, M. Y., Ramadan, D. A., and El-Desouky, B. S. (2024). Inverse power modified Chris-Jerry distribution: properties, estimation, simulation and medical application. Appl. Math. Inf. Sci, 18, 1261-1271.
[8] S. Anatolyev and G. Kosenok. An alternative to maximum likelihood based on spacings. *Econometric Theory*, 21, 472–476 (2005).
[9] A. Asgharzadeh, M. Alizadeh and M. Z. Raqab. Inverse Lindley distribution: Different methods for estimating their PDF and CDF. *J. Stat. Comput. Simul.*, 94, 604–623 (2024).
[10] R. Azimi, M. Esmailian and D. I. Gallardo. The inverted exponentiated Chen distribution with application to cancer data. *Jpn. J. Stat. Data Sci.*, 6, 213–241 (2023).
[11] A. Barbiero and A. Hitaj. Discrete half-logistic distributions with applications in reliability and risk analysis. *Ann. Oper. Res.*, 340, 27–57 (2024).
[12] A. Baricz and T. K. Pogány. Integral and series representations of moment generating functions and their applications. *J. Comput. Appl. Math.*, 386, 113260 (2021).
[13] A. Beghriche et al. The inverse XLindley distribution: Properties and application. *IEEE Access*, 11, 47272–47281 (2023).
[14] F. Buono, E. De Santis, M. Longobardi and F. Spizzichino. Multivariate reversed hazard rates and inactivity times of systems. *Methodol. Comput. Appl. Probab.*, 24, 1987–2008 (2022).
[15] R. C. H. Cheng and N. A. K. Amin. Maximum product spacing estimation with applications. *J. R. Stat. Soc. B*, 45, 394-403 (1983).
[16] M. S. Eliwa, M. El-Morshedy and M. Ibrahim. Inverse Gompertz distribution: Properties and estimation methods. *Ann. Data Sci.*, 6, 321–339 (2019).
[17] M. Evans et al. *Statistical Distributions*. Wiley (2011).
[18] M. N. Faladiba and A. Ahdika. Bayes estimation of survival data. *BAREKENG J. Math. Appl.*, 18, 973–986 (2024).
[19] A. T. Farhat et al. Statistical inference of modified Frechet–Exponential distribution. *Appl. Math. Inf. Sci.*, 17, 109–124 (2023).
[20] K. Ghosh and S. R. Jammalamadaka. A general estimation method using spacings. *J. Stat. Plan. Inference*, 93, 71–82 (2001).
[21] A. J. Gross and V. A. Clark. *Survival distributions: Reliability applications*. Wiley (1975).
[22] J. S. Kamnge and M. Chacko. Half logistic exponentiated inverse Rayleigh distribution: Properties and application to lifetime data. *PLoS ONE*, 20, e0310681 (2025).
[23] P. Kavya and M. Manoharan. A new lifetime model for non-monotone failure rate data. *J. Indian Soc. Probab. Stat.*, 24, 283–310 (2023).
[24] M. Kayid. Statistical inference of quantile past lifetime. *AIMS Math.*, 9, 15346–15360 (2024).
[25] E. H. E. S. Khalifa. *Statistical inference for reliability models*. PhD thesis, Mansoura University, Egypt (2024).
[26] S. D. Krishnarani. On a power transformation of half-logistic distribution. *J. Probab. Stat.*, Article ID 2084236 (2016).
[27] N. Leonenko et al. A class of Rényi information estimators. *Ann. Stat.*, 36, 2153–2182 (2008).
[28] C. T. Lin et al. Inverted gamma as a life distribution. *Microelectron. Reliab.*, 29, 619–626 (1989).
[29] L. Martino and V. Elvira. Metropolis sampling. *Wiley StatsRef*, 1–18 (2017).
[30] R. Millar. *Maximum likelihood estimation and inference*. Wiley (2011).
[31] M. Muhammad and L. Liu. A new extension of generalized half logistic distribution. *Entropy*, 21, 339 (2019).
[32] M. Muhammad et al. Type-I half-logistic distribution: A review. *Austrian J. Stat.*, 52, 34–62 (2023).
[33] N. U. Nair et al. *Quantile-based reliability analysis*. Springer (2013).
[34] A. Papoulis and S. U. Pillai. *Probability, random variables and stochastic processes*. McGraw-Hill (2002).
[35] V. Poynor and A. Kottas. Bayesian inference for mean residual life. *Biostatistics*, 20, 240–255 (2019).
[36] P. L. Ramos, D. Nascimento and F. Louzada. The use of probability distributions in reliability: Applications and estimation. *Appl. Math. Model.*, 77, 1184–1197 (2020).
[37] V. K. Sharma, S. Singh and U. Singh. Generalized inverse Lindley distribution. *Commun. Stat. Theory Methods*, 45, 570–582 (2016).
[38] Q. Tian et al. Prior distributions in reliability applications. *Appl. Stoch. Models Bus. Ind.*, 40, 5–62 (2024).
[39] J. Yu et al. Monitoring inverted exponentiated half logistic quantiles. *J. Appl. Stat.*, 52, 59–96 (2025).

[40] Awajan, M. Y., Ramadan, D. A., Ahmad, H. H., and El-Desouky, B. S. (2025). Applied statistical modeling of infant mortality with the progressively censored IPMCJ distribution. AIMS Mathematics, 10(10), 23880-23918.

[41] A. M. El Gazar, D. A. Ramadan, M. ElGarhy and B. S. El-Desouky. Estimation of parameters for inverse power Ailamujia and truncated inverse power Ailamujia distributions based on progressive type-II censoring scheme. *Innovation in Statistics and Probability*, 1, 76–87 (2025).

[42] Rammadan, D. A., Mohamed El Gazar, A., Hasaballah, M. M., Balogun, O. S., Bakr, M. E., and Alshangiti, A. M. (2025). Modeling Physical and Medical Lifetime Data Using the Inverse Power Entropy Chen Distribution. Mathematics, 13(23), 3743.

[43] H. H. Ahmad and M. M. El-Awady. Reliability Analysis of Multicomponent Stress–Strength Systems Under Progressive First-Failure Censoring Using the Exponentiated Half-Logistic Distribution. *Quality and Reliability Engineering International*, (2026).

[44] H. Ahmad and M. M. El-Awady. Inference and Optimal Design on Partially Accelerated Life Tests for the Power Half-Logistic Distribution Under Adaptive Type II Progressive Censoring. *Mathematics*, 13, 394 (2025).

[45] M. M. El-Awady, M. M. E. Abd El-Monsef and I. M. Elbaz. Exponentiated half-logistic Weibull distribution with reliability inference. *Quality and Reliability Engineering International*, 40, 1875–1903 (2024).

[46] M. M. El-Awady, H. Ahmad, Y. Rabaiah and A. T. Ramadan. The q-Deformed Lindley Distribution: Properties, Statistical Inference, and Applications. *Mathematics*, 14, 1364 (2026).

[47] R. El-Desokey, M. M. El-Awady, H. H. Ahmad and A. El-Gohary. Multicomponent stress-strength reliability inference under progressive Type-II censoring: A one-parameter model with applications to power systems and earthquake data. *AIMS Mathematics*, 11, 8031–8064 (2026).

[48] H. H. Ahmad, M. Aboshady, A. K. Elsherif and D. A. Ramadan. Statistical inference for dependent competing-risk failures in land-based radar detection: A PHW model under generalized progressive hybrid censoring. *AIMS Mathematics*, 10, 15991–16026 (2025).

Abdullah Ghaleb Bani Saleh is currently pursuing a Ph.D. in Mathematical Statistics at Mansoura University, Egypt. He received his B.Sc. degree in 2021 and his M.Sc. degree in 2023 from Al al-Bayt University, Jordan. His research interests include statistical distributions, bivariate distributions, statistical inference, Bayesian statistics, and censoring schemes.

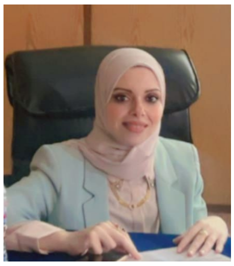

Dina Ahmed Ramadan is an Assistant Professor of Mathematical Statistics at the Department of Mathematics, Faculty of Science, Mansoura University, Egypt. She received her Ph.D. degree from the Faculty of Science, Mansoura University, Egypt, in 2016. Her research interests include statistical inference, estimation theory, Bayesian inference, reliability theory, censored data, life testing, competing risks, masked data, and distribution theory.

Beih El-Sayed El-Desouky received the M.Sc. degree in 1979 and the Ph.D. degree in 1984 in Statistical Mathematics from the Department of Mathematics, Aswan University, Egypt. He is currently a Professor of Mathematical Statistics and Combinatorics at the Department of Mathematics, Faculty of Science, Mansoura University, Egypt.

Mahmoud M. El-Awady is a Lecturer of Mathematics and Statistics in the Basic Sciences Department at the Misr Higher Institute for Commerce and Computers (MET Mansoura), Egypt. His primary research interests lie in the fields of mathematical statistics and data science, with a specific focus on probability distributions, applied statistics, reliability analysis, and estimation theory. He has authored several peer-reviewed articles in reputable international journals, contributing to topics such as lifetime data modeling, Bayesian and non-Bayesian inference, and regression models for bounded response data.